Optical investigations of surface processes in GaP heteroepitaxy on silicon under pulsed chemical beam epitaxy conditions*

U. Rossow,[a] N. Dietz, K. J. Bachmann, and D. E. Aspnes
Physics Department and Materials Science and Engineering, North Carolina State University, Raleigh, North Carolina 27695-8202

(Received 1 March 1996; accepted 4 May 1996)

Surface processes during the heteroepitaxy of GaP on Si under pulsed chemical beam epitaxy conditions were investigated simultaneously by the optical methods reflectance difference/anisotropy spectroscopy, p-polarized reflectance spectroscopy (PRS), and laser light scattering. Our studies were performed during both cyclic and interrupted growth, where the surface was exposed to individual pulses of the precursors triethylgallium (TEG) and tertiarybutylphosphine (TBP). The data show that the three optical probes provide different perspectives of growth. Several surface processes exhibit time constants of the order of 1 s. One such process is the clustering of Ga atoms, or less likely, of TEG fragments, that occurs with TEG exposure. The optical data also show that TBP dealkylation occurs essentially instantaneously upon arrival at the surface, and that TEG dealkylation is the rate-limiting step. The PRS data exhibit fine structure that shows that heteroepitaxial growth can be described by a four-phase model consisting of the substrate, a GaP layer, a surface reaction layer containing all adsorbed species not yet incorporated in the growing layer, and the ambient. By assuming that this surface layer is very thin we derive approximate equations that allow us to treat the PRS response quantitatively. © *1996 American Vacuum Society.*

I. INTRODUCTION

In this article we discuss real-time monitoring of the pulsed chemical beam heteroepitaxial growth of GaP on Si by three different optical techniques: reflectance difference/anisotropy spectroscopy (RDS/RAS),[1–3] p-polarized reflectance spectroscopy (PRS),[4,5] and laser light scattering (LLS).[6] The objective is a better understanding of the growth process, specifically surface chemistry and reaction kinetics. A discussion of the complicated chemistry of this growth system is given in Ref. 7.

The results are expected to be useful in the engineering of heteroepitaxial growth on silicon. In particular, the quality of the heteroepitaxial layers depends strongly on interfacial properties, and can be optimized only when the deposition process, especially the early stage, is well understood. As discussed earlier,[5,8–10] PRS in the visible range shows a large sinusoidal signal during growth due to interference between front- and back-surface reflections associated with the growing GaP layer, from which the overall growth rate can be determined. Superimposed on this is a fine structure that is linked to the pulsed supply of the precursors. This fine structure is also observed in RDS and, to a lesser extent, in LLS. The three probes provide different perspectives of the growth process, and show in particular that in the growth system studied here, triethylgallium (TEG) dealkylation is the rate-limiting step.

II. EXPERIMENT

Heteroepitaxial growth was performed in a pulsed mode at low substrate temperatures of 360–400 °C as measured by thermocouples and calibrated by a pyrometer. The precursors were tertiarybutylphosphine (TBP) and TEG. The silicon substrates were lightly (1–10 Ω cm) p doped. To determine the possible influence of steps on growth, we used (113) substrates and substrates oriented 6° off (001) toward [110]. Since on-axis (001) Si substrates yielded no net RDS signals as a result of the formation of antiphase domains, (001) substrates were used only for comparison.

Details of the RDS configuration are given in Refs. 1 and 2, and those of PRS and LLS in Ref. 5. For PRS and LLS a He–Ne laser was used as light source (633 nm, 1.96 eV). RDS transients were taken at a fixed photon energy of 3.6 eV, where the optical penetration depth of GaP is low and the detected light intensity is high. The intrinsic RDS time resolution was the RDS sampling period, 1 ms. However, to improve signal-to-noise ratios we averaged 25 and 50 points for interrupted and cyclic growth, respectively, yielding effective time resolutions of 25 and 50 ms, respectively. The time resolution for PRS and LLS was 100 ms. The pneumatic switching valves for TEG and TBP have a small dead volume and a time response faster than 20 ms, as specified by the manufacturer (NUPRO).

III. LINEARIZATION OF THE PRS SIGNAL

A typical PRS transient for a GaP layer heteropitaxially grown on Si is shown in Fig. 1. These data can be described with the so-called four-phase model, which involves the ambient (0), a surface reaction layer (1), the GaP layer (2), and the Si substrate (3), where all interfaces are assumed to be sharp and reflections from the back of the substrate can be ignored.[11] It is necessary to include a surface reaction layer, because unreacted species on the surface of the growing GaP film generally have refractive indices different from that of

*Published without author corrections.
[a]Electronic mail: rossow@unity.ncsu.edu

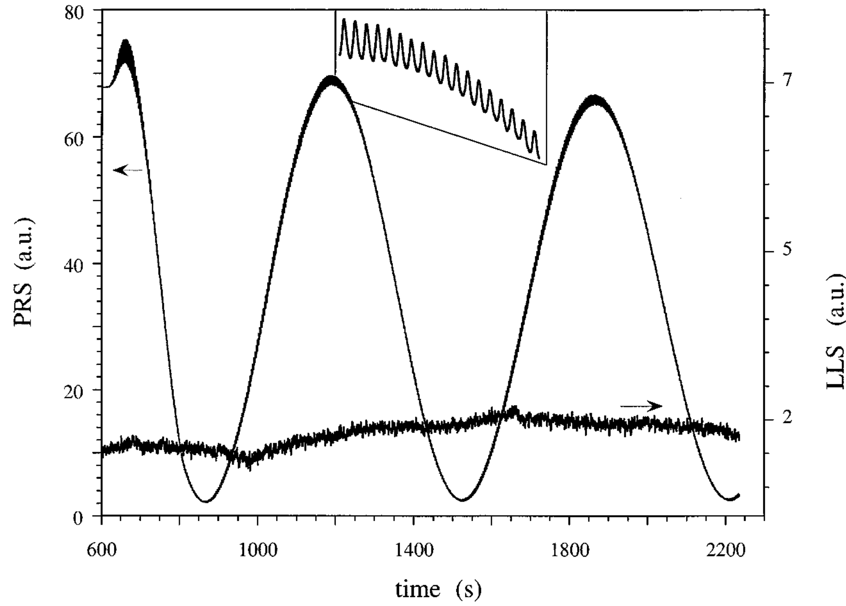

FIG. 1. Typical PRS transient during heteroepitaxial growth on Si. The fine structure is shown on an expanded scale in the inset. The nonzero values of the minima are due to an offset in the electronic signal.

GaP. This is manifest by the data of Fig. 1, which show a fine structure in the PRS data that accompanies cyclic changes in ambient exposure.

In the four-phase model the PRS signal is proportional to the absolute square $R_{4p}=|r_{4p}|^2$ of the complex reflectance coefficient r_{4p} for p-polarized light, which is given by[12]

$$r_{4p}=\frac{(r_{01p}+r_{12p}e^{i2\beta_1})+(r_{01p}r_{12p}+e^{i2\beta_1})r_{23p}e^{i2\beta_2}}{(1+r_{01p}r_{12p}e^{i2\beta_1})+(r_{12p}+r_{01p}e^{i2\beta_1})r_{23p}e^{i2\beta_2}}, \quad (1)$$

where

$$\beta_i=\frac{2\pi d_i}{\lambda}\sqrt{\epsilon_i-\sin^2\theta_0}, \quad i=1,2 \quad (2)$$

and where θ_0 is the angle of incidence. Since the surface reaction layer is thin ($|\beta_1|\ll 1$), we can linearize Eq. (1) with respect to β_1 as

$$r_{4p}(\beta_1)=r_{4p}(\beta_1=0)+\beta_1\left.\frac{\partial r_{4p}}{\partial\beta_1}\right|_{\beta_1=0}$$

$$=r_{4p0}+\beta_1\left.\frac{\partial r_{4p}}{\partial\beta_1}\right|_{\beta_1=0}. \quad (3)$$

The first term on the right side of Eq. (3) describes interference due to the growing GaP layer and the second the fine structure due to the variation of d_1 or ϵ_1 with exposure.

The interference term r_{4p0} is given by

$$r_{4p0}=\frac{r_{02p}+r_{23p}e^{i2\beta_2}}{1+r_{02p}r_{23p}e^{i2\beta_2}}. \quad (4)$$

If the Brewster condition $\theta_0=\theta_B$ is fulfilled exactly, then $r_{4p0}=r_{03p}=0$ when $\exp(i2\beta_2)=1$ and therefore $r_{02p}=-r_{23p}$. Under this condition

$$r_{4p0}=r_{02p}\frac{1-e^{i2\beta_2}}{1-|r_{02p}|^2e^{i2\beta_2}} \quad (5)$$

$$\approx -2ir_{02p}e^{i\beta_2}\sin\beta_2. \quad (6)$$

For real β_2 we therefore have

$$\text{PRS signal}\sim R_{4p0}=|r_{4p0}|^2=4R_{02p}\sin^2\beta_2, \quad (7)$$

where $R_{02p}=|r_{02p}|^2$. Thus for $\theta_0=\theta_B$ and $\beta_1=0$ the PRS signal exhibits a sinusoidal behavior with a period $\Delta d=\lambda/2(\epsilon_2-\sin^2\theta_0)^{-1/2}$. For GaP at 632.8 nm [$\epsilon_{\mathrm{GaP}}=10.96+i0.00$ (see Ref. 13)] and $\theta_0=70°$, Δd is approximately 101 nm.

For growth monitoring the Brewster condition is difficult to realize because the dielectric function, and consequently θ_B, is temperature dependent. For the more general case of $\theta_0\approx\theta_B$, R_{4p0} is given by

$$R_{4p0}\approx R_{03p}+2[R_{23p}-\mathrm{Re}(r^*_{03p}r_{23p})]-2\cos 2\beta_2[R_{23p}-\mathrm{Re}(r^*_{03p}r_{23p})]-2\sin 2\beta_2\,\mathrm{Im}(r^*_{03p}r_{23p}), \quad (8)$$

where the R_{ijp} terms have obvious meaning. If the substrate is weakly absorbing, as is the case for Si at 632.8 nm, the last term can be neglected and we obtain

$$R_{4p0}\approx R_{03p}+2[R_{23p}-\mathrm{Re}(r^*_{03p}r_{23p})][1-\cos 2\beta_2], \quad (9)$$

which is basically Eq. (7) with a dc offset $R_{03}\geq 0$, as seen in Fig. 1. If $R_{03}=0$ ($\theta=\theta_B$) then from either Eq. (7) or (9) the PRS signal must begin to rise when GaP growth is initiated. However, Fig. 1 shows that this is not observed: the signal begins near its maximum and then decreases. From Eq. (9) this is possible if $R_{03}\neq 0$ and $r_{23p}<r_{03p}$, which means that $[R_{23p}-\mathrm{Re}(r^*_{03p}r_{23p})]<0$. Furthermore, with increasing thickness of the GaP layer we observe that the signal ap-

proaches zero. Therefore, $R_{03p}\approx 4|R_{23p}-\mathrm{Re}(r_{03p}^{*}r_{23p})|$. From this result it follows that $r_{03p}\approx 2r_{23p}$. Using these conditions and the values for the dielectric functions of Si and GaP given above, we can calculate θ_0. We find this to be about 70.4°, which is slightly less than θ_B.

To determine the fine-structure contribution we must evaluate the β_1 scaling factor

$$\left.\frac{\partial r_{4p}}{\partial \beta_1}\right|_{\beta_1=0}=\frac{2i(1-r_{01p}^2)/r_{12p}}{(1+r_{01p}r_{12p})^2}\times\frac{(1+r_{23p}e^{i2\beta_2})^2+r_{23p}e^{i2\beta_2}\left(\frac{1+r_{12p}^2}{r_{12p}}-2\right)}{(1+r_{02p}r_{23p}e^{i2\beta_2})^2}. \tag{10}$$

For $\theta_0\approx\theta_B$, r_{02p} and r_{23p} are small compared to 1 [≈ 0.083 and 0.072, respectively, for $\theta_0=70°$ and $\epsilon_{\mathrm{Si}}=15.07+i0.15$) [see Ref. 13]. Neglecting products of these terms yields

$$\left.\frac{\partial r_{4p}}{\partial \beta_1}\right|_{\beta_1=0}\approx\frac{2i(1-r_{01p}^2)}{(1+r_{01p}r_{12p})^2}\,[r_{12p}+r_{23p}e^{i2\beta_2}(1+r_{12p}^2)]. \tag{11}$$

The term in the brackets can be given a simple geometric interpretation. In the transparent region of GaP, β_2 is real. Therefore, with increasing layer thickness $e^{i2\beta_2}$ describes a circle of unit radius in the complex plane. If the surface reaction layer is also transparent, r_{12p} is also real and the term in the brackets is largest/smallest for $e^{i2\beta_2}=\pm 1$ depending on the sign of r_{12p} and r_{23p}. Since for $e^{i2\beta_2}=\pm 1$ the interference term shows extrema the fine structure will be largest/smallest at the minima/maxima of the PRS signal (see Fig. 1). This effect is most pronounced when $r_{12p}\approx r_{23p}(1+r_{12p}^2)$, a condition that is fulfilled for reasonable values of ϵ_1 (for example, for $\epsilon_1=8$ the two terms are nearly equal). For small surface absorption we can write $r_{12p}=|r_{12p}|(1+i\delta)$, where $\delta\ll 1$. Then

$$[r_{12p}+r_{23p}e^{i2\beta_2}(1+r_{12p}^2)]\sim[|r_{12p}|+i|r_{12p}|\delta+r_{23p}e^{i2\beta_2}(1+|r_{12p}|^2)], \tag{12}$$

where the term $\delta r_{23p}|r_{12p}|^2$ can be neglected. Now the center of the circle with radius $r_{23p}(1+|r_{12p}|^2)$ is located a distance $|r_{12p}|$ on the real axis and $\delta|r_{12p}|$ above the real axis. The amplitude of the fine structure reaches its maximum value at $\tan 2\beta_2=|r_{12p}|\delta/(r_{23p}[1+|r_{12p}|^2])$. This no longer coincides with the extrema of the interference term. Therefore, from the relative phases of the interference and fine-structure signals we can obtain information about $\mathrm{Im}(r_{12p})$, and thus the surface absorption.

If $\mathrm{Im}(r_{12p})\gg\mathrm{Re}(r_{12p})$, which is the case for a metallic surface layer with $\mathrm{Re}(\epsilon_1)<0$, $\mathrm{Im}(\epsilon_1)>0$, no phase matching of r_{12p} and $r_{23p}[1+r_{12p}^2]$ can occur. However, if $\mathrm{Re}(r_{12p})\ll 1$ then we again obtain the equation of a circle, but one with its center near the imaginary axis.

Combining the previous results the general expression for the PRS signal, to first order in β_1, is

$$\mathrm{PRS}\sim R_{4p}\approx R_{4p0}+2\,\mathrm{Re}\left[r_{4p0}^{*}\beta_1\left.\frac{\partial r_{4p}}{\partial\beta_1}\right|_{\beta_1=0}\right]. \tag{13}$$

Therefore, the amplitude of the fine structure that is caused by a variation of β_1, i.e., variations in ϵ_1 and/or d_1, depends also on r_{4p0}^{*} and $\partial r_{4p}/\partial\beta_1|_{\beta_1=0}$. Neglecting for simplicity the squared terms of the Fresnel coefficients we obtain

$$\mathrm{PRS}\sim R_{4p}\approx R_{03p}+2[R_{23p}-\mathrm{Re}(r_{03p}^{*}r_{23p})][1-\cos 2\beta_2]\times\mathrm{Re}\{r_{02p}(1-e^{-i2\beta_2})\beta_1 2i[r_{12p}+r_{23p}e^{i2\beta_2}\times(1+r_{12p}^2)]\}. \tag{14}$$

Therefore, the amplitude of the fine structure is also periodic in $2\beta_2$. In general, the situation is complicated because the fine-structure term is multiplied by real and imaginary parts of r_{4p0}^{*}, which results in terms $(1-\cos 2\beta_2)$ and $\sin 2\beta_2$ that are not in phase. For one extremum $2\beta_2=\pi$, in which case

$$2\,\mathrm{Re}\left[r_{4p}^{*}(\beta_1=0)\beta_1\left.\frac{\partial r_{4p}}{\partial\beta_1}\right|_{\beta_1=0}\right]=-r_{02p}\frac{16\pi d}{\lambda}[\mathrm{Re}(\sqrt{\epsilon_1-\sin^2\theta_0})\times\mathrm{Im}(r_{12p}-r_{23p}[1+r_{12p}^2])+\mathrm{Im}(\sqrt{\epsilon_1-\sin^2\theta_0})\times\mathrm{Re}(r_{12p}-r_{23p}[1+r_{12p}^2])]. \tag{15}$$

This vanishes for real ϵ_1. The same occurs for $2\beta_2=0$. In contrast, we often observe that the fine structure is largest near the maxima of PRS signals. Consequently, in these cases $\mathrm{Im}(\epsilon_1)$ must be significant. This also follows directly from Eq. (1). At the extrema, $\exp(i2\beta_2)=\pm 1$, and for GaP on Si at 632.8 nm all Fresnel coefficients are real. Then the absolute value of r_{4p} contains only terms in $\cos 2\beta_1$, which is quadratic in β_1. We note also that for both parts of the PRS signal the zero-order term due to interference, $|r_{4p}(\beta_1=0)|^2$, and the fine structure term, $2\,\mathrm{Re}[r_{4p}^{*}(\beta_1=0)\beta_1(\partial r_{4p}/\partial\beta_1)|_{\beta_1=0}]$, are both of the order of the square of the Fresnel coefficient. Therefore, the large descrepancy in value between the two terms can only be explained by β_1 being small as suggested above. The ratio in the maxima is approximately

$$2\,\mathrm{Re}\left[r_{4p}^{*}(\beta_1=0)\beta_1\left.\frac{\partial r_{4p}}{\partial\beta_1}\right|_{\beta_1=0}\right]\Big/|r_{4p}(\beta_1=0)|^2=-1/r_{02p}\frac{4\pi d}{\lambda}[\mathrm{Re}(\sqrt{\epsilon_1-\sin^2\theta_0})\times\mathrm{Im}(r_{12p}-r_{23p}[1+r_{12p}^2])+\mathrm{Im}(\sqrt{\epsilon_1-\sin^2\theta_0})\times\mathrm{Re}(r_{12p}-r_{23p}[1+r_{12p}^2])]. \tag{16}$$

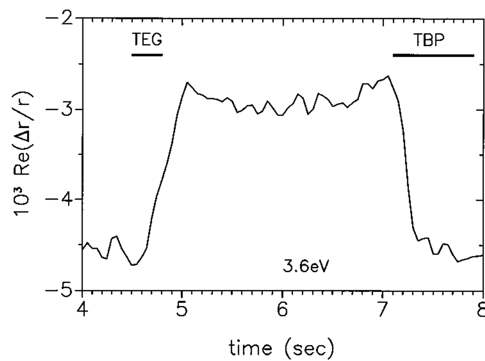

FIG. 2. RDS transient at 3.6 eV for one exposure cycle during heteroepitaxial growth of GaP on a vicinal wafer orientated 6° off (001) toward [110]. The response to the TEG pulse is slower than that to the TBP pulse. The upper level is not flat but has overlaid structure.

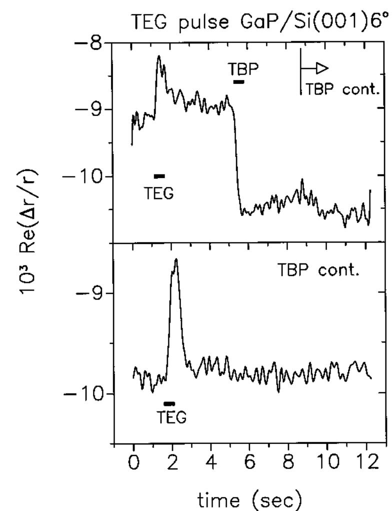

FIG. 3. Comparison between RDS responses to a single pulse of TEG on a surface oriented 6° off (001) toward [110], where the TBP exposure is either continuous (lower panel) or pulsed (upper panel). All pulse durations were 0.5 s, as indicated by the solid bars. With continuous TBP exposure the baseline is essentially invariant, indicating that the surface recovers quickly after the TEG pulse.

From Fig. 1 this ratio is 0.02. If we assume that the real and imaginary parts of $(r_{12p}-r_{23p}[1+r_{12p}^2])$ are of the order of $1/r_{02p}$, which is a crude approximation, and neglect $\sin^2\theta_0$ the ratio becomes

$$\frac{4\pi d}{\lambda}[\mathrm{Re}(\sqrt{\epsilon_1})+\mathrm{Im}(\sqrt{\epsilon_1})]. \tag{17}$$

If we further assume that d is about 0.5 nm, then $4\pi d/\lambda$ is 0.01 and $[\mathrm{Re}(\sqrt{\epsilon_1})+\mathrm{Im}(\sqrt{\epsilon_1})]$ is of the order of 2. This sets upper limits of 10 to the imaginary and absolute values of the real part of ϵ_1.

Although our motivation for this analysis is the understanding of the PRS data for GaP on Si, this analysis holds in general for any heterostructure where the epitaxial layer has a high refractive index and is not optically absorbing.

IV. RESULTS AND DISCUSSION

In the following we discuss the results of three different types of experiments: continuous cyclic growth, single pulses of TEG during continuous TBP exposure, and single pulses of both TEG and TBP. These experiments were performed for (113) surfaces and surfaces cut 6° off (001) toward [110] as indicated either in the figures or in the captions. Similar results were obtained for both orientations. So far, we have found no evidence of a growth dependence on step density.

A. Continuous cyclic growth

Figure 2 shows a typical RDS transient obtained at 3.6 eV and 25 ms averaging for a single 4 s cycle of alternating TEG and TBP exposures during the growth of GaP on a Si surface oriented 6° off (001) toward [110]. At 3.6 eV this GaP layer is optically thick. The onsets of the rising and falling parts of the transient correlate with the onsets of TEG and TBP exposures, respectively, but the rising and falling durations do not coincide with precursor exposures. Although TEG exposure was 0.3 s the rise time is broadened to about 0.5 s, whereas the decay time is less than 0.25 s for a TBP pulse of 0.8 s. An overshoot also appears on both rising and falling edges. The difference between response and exposure times are likely caused by surface processes.

B. Single precursor pulses

To investigate this behavior further we applied single 0.3 and 0.5 s TEG pulses to freshly grown GaP annealed at the growth temperature by a continuous or pulsed supply of TBP. The RDS response to a 0.5 s TEG pulse during TBP exposure for a surface annealed in TBP for 54 s following growth is shown in the lower panel of Fig. 3. At this point TBP exposure was terminated but the molecular hydrogen flow remained. The upper panel shows the result obtained when this surface was exposed to TEG followed 4 s later by a TBP pulse and 2.5 s later by continuous exposure to TBP. A repeat of this sequence yielded the same results except that the starting level was lower than that shown in the upper panel of Fig. 3. This level shift indicates that the surface becomes Ga rich when TBP exposure is terminated.

The RDS response to TEG clearly depends on whether TBP exposure is interrupted or continuous. With continuous TBP exposure the RDS signal increases linearly during the TEG pulse and afterward decays exponentially to its starting value. With interrupted TBP exposure a TEG pulse generates a fast (rise time <0.25 s) response followed by an exponential decay of time constant of about 0.7 s to a level higher than the original baseline. The original baseline is recovered only after further TBP exposure. We expect that the change of the RDS signal is related to the total amount of Ga present on the surface. If we take the RDS signal of the phosphorous-rich, TBP-annealed surface as the reference, the change in the RDS signal after TBP exposure in the upper transient ($t\approx5$ s) is within 20% of the change induced by

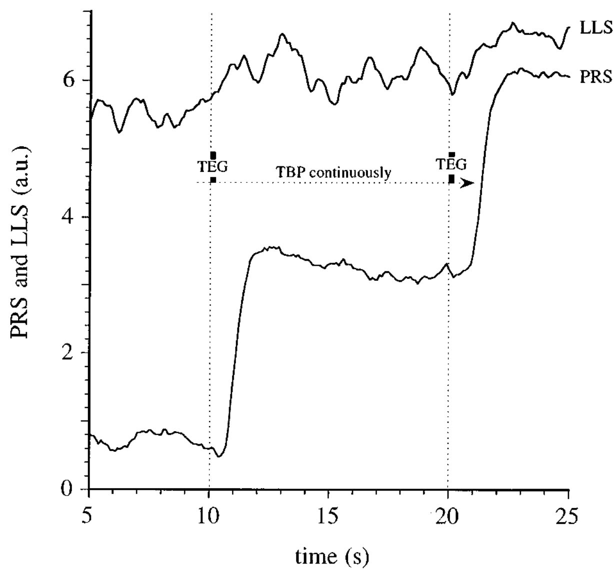

FIG. 4. Typical PRS and LLS transients for TEG pulses for a (113) surface under continuous exposure to TBP.

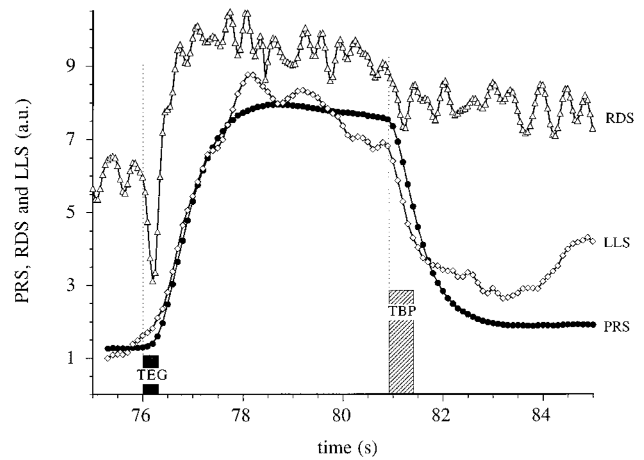

FIG. 5. Comparison of PRS, LLS, and 3.6 eV RDS responses upon exposure of a (113) surface to a TEG pulse followed by a TBP pulse.

TEG for continuous TBP exposure in the lower transient. It is also comparable to the change in signal for continuous cyclic growth when TBP is pulsed (see Fig. 2).

The PRS and LLS data provide another perspective of these processes, as illustrated in Fig. 4. For continuous TBP exposure the scattered light intensity increases only slightly if at all following a TEG pulse, while the PRS transient exhibits steplike behavior. From Eq. (7) we know that during steady-state growth, the increasing film thickness yields a sinusoidal PRS response, which is a much weaker edge than observed. We can therefore conclude that more than one process is active on the surface. This is further supported by the surprising fact that Ga does not begin to be incorporated into the GaP layer until after the TEG pulse is complete. This is not in contradiction to the faster RDS response of Fig. 2, because at 3.6 eV RDS is sensitive only to changes of surface anisotropy and not to layer thickness.

More insight into these processes can be obtained by examining responses to separate pulses of TEG and TBP. In Fig. 5 we compare LLS, PRS, and RDS transients for separate TEG and TBP pulses for GaP layers grown on (113) Si surfaces. As with (001) surfaces TEG exposure results in a broad feature in all three sets of data. However, the onsets for the LLS and PRS responses are delayed substantially with respect to that of the TEG pulse. However, at substrate temperatures well below those used for normal growth, an immediate PRS and LLS response was obtained. Under present conditions a TBP pulse generates an immediate exponential decay in the PRS and LLS transients while the RDS signal recovers essentially linearly within 0.4 s. As shown in Fig. 6 the PRS and LLS decays are well described by exponentials with time constants of 0.54 and 0.70 s, respectively. The RDS transient is more complicated and is discussed below.

Since the TEG pulse length was 0.5 s and the PRS and LLS responses occurred after the TEG pulse had terminated, the PRS and LLS delay times are at least 0.5 s. Since this delay time is much longer than the specified response time of the valves and since the response to TBP exposure is effectively immediate, the results show that rate-limiting intermediate surface processes are involved. Light scattering is caused by structures on the surface with a characteristic length, i.e., a feature size or separation, of order λ (here 632.8 nm), which are removed or smoothed by exposure to TBP. The reflectance of the material in these structures is probably rather high because it is very unlikely that these structures are large but instead should have diameters of the order of a few nm. Since the refractive index of TEG is low—smaller than 1.002 for the atmospheric-pressure gas phase[14]—and TEG is unstable at the temperatures used here, the delayed LLS response indicates that the LLS signal is

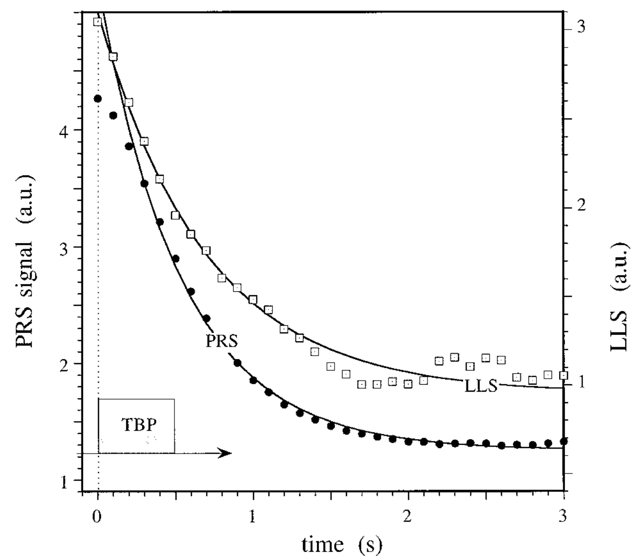

FIG. 6. Exponential fit to the PRS and LLS decay transients after TBP exposure for a (113) surface with a pulse sequence similar to that used in Fig. 5.

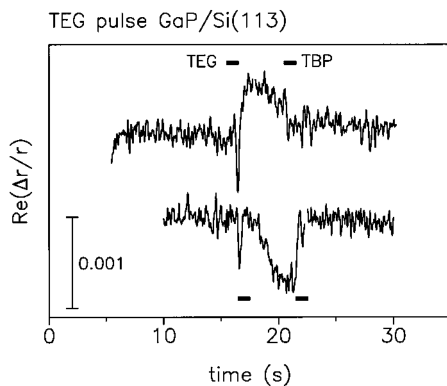

FIG. 7. Two RDS transients for a (113) surface annealed for 30 s in TBP followed by the same pulse sequence as in Fig. 5.

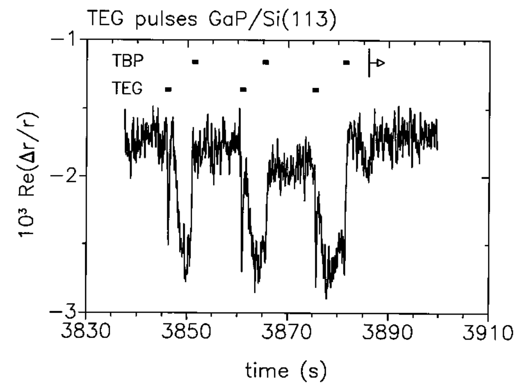

FIG. 8. RDS transients for a (113) surface for various combinations of TEG and TBP pulses followed by continuous TBP exposure.

due to the formation of Ga-containing clusters. The most likely constituent is metallic Ga, since neither monoethylgallium (MEG) nor diethylgallium (DEG) are likely to aggregate. Furthermore, even in liquid-phase densities their refractive indices should not exceed 1.5, which is too small to explain the LLS signal. However, the species that diffuse to form the clusters may be MEG, DEG, or even TEG, with complete dealkylization occurring only after the molecule arrives at the cluster. If MEG is the diffusing species, the fact that all its outer electrons are in filled orbitals suggests that it is relatively stable and hence there exists some probability that it could also desorb.

In this picture the delayed onset of the LLS and PRS responses would be due to complete and partial TEG dealkylization, which at the low pressures (low 10^{-5} mbar) and substrate temperatures (typically around 360 °C) used here is expected to occur on the surface instead of in the gas phase. The Ga-rich clusters remain stable because the incorporation of Ga as GaP requires the presence of P.

Although the LLS and PRS signals are related their origins are different. For sufficiently low TEG exposures the LLS signal vanishes but a strong PRS response remains. Moreover, depending on the thickness of the GaP layer and therefore the phase shift of the electromagnetic wave within the layer, the peaklike feature in the PRS transient due to the TEG pulse can be inverted as discussed above in the context of Eq. (11). Consequently, it is likely that the PRS signal is caused by a thin surface layer whose dielectric function differs strongly from that of the underlying film.

Figure 7 shows two RDS responses for a TEG pulse obtained on a GaP layer grown on a (113) Si surface. The lower transient is taken at a later time but under otherwise identical conditions. Clearly, each transient has at least two components. One is a brief negative spike representing a fast process that lasts less than 0.5 s. The other is a broad feature between the negative spike and the TBP pulse that is similar to that observed in PRS and LLS. The shape of the broad feature is history dependent, and unlike the negative spike it can appear either above or below the TBP-established base line. This variation of level cannot be due to interference from a backreflected wave within the GaP layer, as is the case for PRS, since at 3.6 eV the 20 nm penetration depth is much smaller than the layer thickness. Also, this behavior cannot be explained by surface chemistry alone, because if the surface only changes between P-rich and Ga-rich conditions the final state should be similar for the two transients. However, it is well known that the presence of anisotropic structures on the surface, for example ellipsoidal clusters, cause large RDS responses,[15] with the RDS signal depending on the shape and the optical properties of the clusters. For randomly distributed isotropic clusters the RDS signal must vanish by symmetry. A broad RDS response could be explained by supposing that initially isotropic clusters become anisotropic. The cluster material itself is not expected to be anisotropic since bulk Ga is liquid at the growth temperature. We also observe a change in the corresponding PRS transient.

Curiously, the sharp negative spike does not always appear at the onset of TEG exposure but, as shown in Fig. 8, is further delayed with successive TEG/TBP cycles. The TBP-established baseline also decreases with successive cycles, recovering only upon continuous exposure to TBP, as also shown in Fig. 8. This indicates that the surface retains some morphology remnant or fraction of fully or partially dealkylized TEG. The recovery effect of continuous TBP exposure is most pronounced in Fig. 9, where a steplike transient is observed.

C. Possible surface processes

It is puzzling that surfaces being continuously exposed to TBP react much more slowly to TEG than when TBP exposure is interrupted. No such variation is observed for TBP: the PRS, LLS, and RDS data all show that TBP appears to react immediately upon reaching the surface, regardless of its initial state. In particular, no LLS response would be expected if TBP were only physisorbed on the surface, since the refractive index of TBP is small. One possible explanation for the slower TEG response with TBP coexposure is that the butyl group requires time to desorb. The butyl group probably does not desorb directly as a radical or as fragments. Because the butyl group is also very bulky, it is also

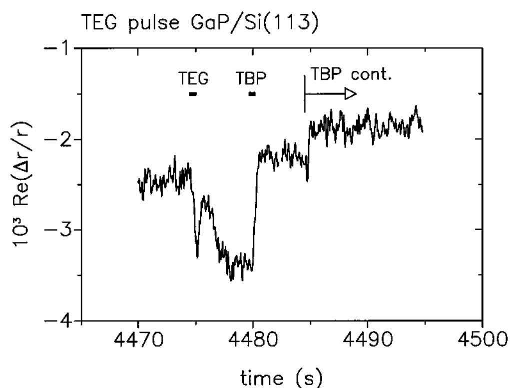

FIG. 9. As in Fig. 8 but after further deposition of GaP. A steplike response occurs when TBP exposure becomes continuous.

unlikely that two butyl groups will react or that butyl groups are incorporated into the growing layer. Most likely the butyl groups will react with hydrogen that originates from either (i) PH_2, (ii) the butyl group itself by conversion to t-butene (C_4H_8), or (iii) β-exchange within the ethyl groups to form C_2H_4. Hence, the likely possibilities are that (1) butyl reacts with atomic hydrogen at the surface, desorbing as t-butane or (2) t-butene is formed directly. In the former case we can expect that the attachment of TEG or its fragments to the P sites will be delayed. A similar argument should hold for TBP.

For surfaces terminated by P, one P bond is unsaturated. Two neighboring P atoms may form a dimer, or the dangling bond can be saturated by hydrogen. It is not clear at present whether hydrogen desorbs from the surface at these growth temperatures. However, the behavior of Si surfaces may give some hints about the nature of the P dangling bond. The Si dimer bond is strong and the desorption temperature of H from the dihydride phase is lower (about 300 °C) than that of H from the monohydride phase (around 520 °C). Since P has a lone pair orbital, a P-rich surface terminated by H should more closely resemble the Si dihydride than the Si monohydride. Growth temperatures near 360 °C are therefore above the temperature for H desorption. Hydrogen desorption may proceed in three ways: (1) as H_2; (ii) as ethane formed by β-exchange within the ethyl group; and (iii) as t-butane (C_4H_{10}) by saturation within the butyl group. However, in all cases all surface dangling bonds are saturated and the surface is passivated in a manner similar to that of As-terminated Si.[16,17]

V. SUMMARY AND CONCLUSIONS

Comparison of RDS, PRS, and LLS data for exposure of GaP layers grown on vicinal (001) and (113) Si surfaces to single pulses of TEG and TBP reveals that RDS, PRS, and LLS deliver complementary information, a necessary prerequisite for an unambigious interpretation of growth mechanisms. However, the observed chemistry is very complex. Further investigations using a quadrupole mass spectrometer in addition to the optical probes and an optical multichannel analyzer (OMA) detection system to obtain PRS spectra are in progress.

We have derived linearized expressions for the fine structure in the PRS data, which shows that a reaction layer including all not-yet-incorporated surface species is present on the surface of the growing GaP layer. This reaction layer is optically absorbing for the wavelengths used here. The time constants of the surface reaction processes preceding Ga and P incorporation are of the order of 1 s under present conditions, and appear to be substantially faster for TBP than for TEG. At least two processes occur when the surface is exposed to TEG. From LLS data we find evidence for Ga clustering, which is consistent with the observation that the surface reaction layer is optically absorbing. Unreacted species that are not directly incorporated into the growing layer also remain on the surface possibly for tens of seconds. For this system we find no evidence for atomic layer epitaxy, i.e., that growth is self-limiting. Our results are not specific to GaP on Si and are equally valid for GaP homoepitaxy as well. We expect that the ternary system $Ga_xIn_{1-x}P$ will behave similarly.

ACKNOWLEDGMENTS

This work was supported by the Alexander von Humboldt Foundation, the Office of Naval Research under Contract No. N-00014-93-1-0255, ARPA/AFOSR Grant No. F49620-95-1-0437, and DOD/AFSOR MURI Grant No. F49620-95-1-0447.

[1] D. E. Aspnes, J. Vac. Sci. Technol. B **3**, 1498 (1985).
[2] D. E. Aspnes, J. P. Harbison, A. A. Studna, L. T. Florez, and M. K. Kelly, J. Vac. Sci. Technol. A **6**, 1327 (1988).
[3] W. Richter, Philos. Trans. R. Soc. London Ser. A **344**, 453 (1993).
[4] N. Dietz, A. Miller, J. T. Kelliher, D. Venables, and K. J. Bachmann, J. Cryst. Growth **150**, 691 (1995).
[5] N. Dietz, U. Rossow, D. E. Aspnes, and K. J. Bachmann, J. Electron. Mater. **24**, 1569 (1995).
[6] D. J. Robbins, A. J. Pidduck, C. Pickering, I. M. Young, and J. L. Glasper, Proc. SPIE **1002**, 25 (1988).
[7] K. J. Bachmann, U. Rossow, N. Sukidi, H. Castleberry, and N. Dietz, J. Vac. Sci. Technol. **14**, 3019 (1996).
[8] K. J. Bachmann, U. Rossow, and N. Dietz, Mater. Sci. Eng. B **35**, 472 (1995).
[9] N. Dietz, U. Rossow, D. E. Aspnes, and K. J. Bachmann, J. Cryst. Growth (in press).
[10] N. Dietz, U. Rossow, D. E. Aspnes, and K. J. Bachmann, Appl. Surf. Sci. (in press).
[11] N. Dietz and K. J. Bachmann, Vacuum **47**, 133 (1996).
[12] R. M. A. Azzam and N. M. Bashara: *Ellipsometry and Polarized Light* (North-Holland, Amsterdam, 1977).
[13] D. E. Aspnes and A. A. Studna, Phys. Rev. B **27**, 983 (1983).
[14] Refractive indices of gases with similar attached groups are well below 1.002. See *Handbook of Chemistry and Physics*, 64th ed. (Chemical Rubber, Boca Raton, FL, 1983), p. E-365.
[15] E. Steimetz, T. Zettler, W. Richter, D. I. Westwood, D. A. Woolf, and Z. Sobiesierski, J. Vac. Sci. Technol. **14**, 3058 (1996).
[16] R. D. Bringans, Crit. Rev. Solid State Mater. Sci. **17**, 353 (1992).
[17] U. Rossow, U. Frotscher, W. Richter, and D. R. T. Zahn, Surf. Sci. **287/288**, 718 (1993).